Bacterial carbon production in Lake Erie is influenced by viruses and solar radiation

Steven W. Wilhelm and Ralph E.H. Smith

Abstract: Bacterial production is an integral recycling mechanism that facilitates carbon flow through aquatic food webs. Factors influencing bacterial activity therefore impact carbon flow. Although ecologists consider grazing and dissolved organic carbon flux to be the major regulators of bacterial activity, we explored two other important pressures. Virus-like particle abundance ranged from 3.7×10^{10} to $37.9 \times 10^{10} \cdot L^{-1}$ in samples collected during August 1997 and July 1998. Bacterial abundance during these periods ranged from 1.8×10^{9} to $4.6 \times 10^{9} \cdot L^{-1}$. Based on electron microscopic analysis, viruses in Lake Erie would have been responsible for 12.1–23.4% of bacterial mortality and, in quasi-steady-state conditions, a comparable loss of bacterial productivity. In the central basin, solar radiation was also demonstrated to regulate bacterial productivity. Ultraviolet radiation (295–400 nm) was shown to inhibit bacterial productivity according to a cumulative exposure kinetic model, and biological weighting functions were derived to enable calculation of time- and depth-integrated photoinhibition. The daytime photoinhibitory loss of bacterial carbon production was estimated to be 14–30% over the upper 5 m, primarily due to ultraviolet radiation >320 nm. Viruses and sunlight are therefore of comparable importance as regulators of bacterial activity in this system.

Résumé : La production bactérienne constitue un mécanisme de recyclage intégral qui facilite le flux de carbone dans les réseaux alimentaires aquatiques. Les facteurs qui influent sur l'activité bactérienne ont donc un impact sur le flux de carbone. Les écologistes considèrent que le broutage et le flux de carbone organique dissous sont les principaux régulateurs de l'activité bactérienne, mais nous examinons ici deux autres facteurs importants. Dans des échantillons recueillis en août 1997 et en juillet 1998, l'abondance des particules viroïdes était de 3,7 à $37,9 \times 10^{10} \cdot L^{-1}$. L'abondance des bactéries dans ces périodes était de 1,8 à $4,6 \times 10^{9} \cdot L^{-1}$. Selon des analyses par microscopie électronique, les virus dans le lac Érié auraient été responsables de 12,1 à 23,4% de la mortalité bactérienne, et dans des conditions d'équilibre presque complet, d'une réduction comparable de la productivité bactérienne. Dans le bassin central, on a montré que le rayonnement solaire régulait aussi la productivité bactérienne. On a montré que le rayonnement ultraviolet (UV, 295–400 nm) inhibait la productivité bactérienne suivant un modèle cinétique d'exposition cumulative, et on a établi des fonctions de pondération biologique pour calculer la photo-inhibition en fonction du temps et de la profondeur. On a estimé que la réduction de la production de carbone bactérien par photo-inhibition était de 14 à 30% dans les premiers 5 m de la colonne d'eau, les UV de plus de 320 nm en étant les principaux responsables. Les virus et le rayonnement solaire sont donc des régulateurs de l'activité bactérienne d'égale importance dans ce système.

[Traduit par la Rédaction]

Introduction

The Great Lakes basin is home to 33 million people, including >10% of the population of the United States and >30% of the population of Canada. The lakes themselves constitute the largest system of fresh, surface water on earth, containing about 20% of the world's supply. Lake Erie, arguably the most human-influenced of all the Great Lakes, is composed of three distinct basins with a systematic gradient in trophic status from west to east along the length of the lake (Mortimer 1987). Despite its reputation as a eutrophic lake, Lake Erie now varies from mesotrophic (at its western extremity) to oligotrophic, due to phosphorus controls and enhanced benthic filtering activity by exotic mussels of the genus *Dreissena* (e.g., Nicholls and Hopkins 1993). In fact, concern now exists that the lake may not be sufficiently productive to support the fisheries that have developed over recent decades. To assess such concerns and evaluate potential compensatory measures, we first need a more comprehensive understanding of the entire aquatic food web and its linkages to nutrient cycles. A key weakness at present in the Great Lakes, and perhaps in large lakes generally, is our understanding of their microbial ecology.

Viruses are pervasive components of aquatic systems (see Maranger and Bird 1995; Wilhelm and Suttle 1999). Understanding their role in the mortality of bacteria and recycling of carbon, nutrient, and energy flow through aquatic systems is of critical importance to understanding how these systems work. At present, there is relatively little information on viral abundance for freshwater systems (Weinbauer and Höfle 1998*a*, 1998*b*). Bacterial production rates themselves are not well known for Lake Erie, although bacterial production has been shown at times to rival autotrophic production in other parts of the Great Lakes system (e.g., Scavia and Laird 1987).

Received March 16, 1999. Accepted September 24, 1999. J15065

S.W. Wilhelm.[1] Department of Microbiology, University of Tennessee, Knoxville, TN 37996, U.S.A.
R.E.H. Smith. Department of Biological Sciences, University of Waterloo, Waterloo, ON N2L 3G1, Canada.

[1]Author to whom all correspondence should be addressed. e-mail: wilhelm@utk.edu

Fig. 1. Location of stations in Lake Erie.

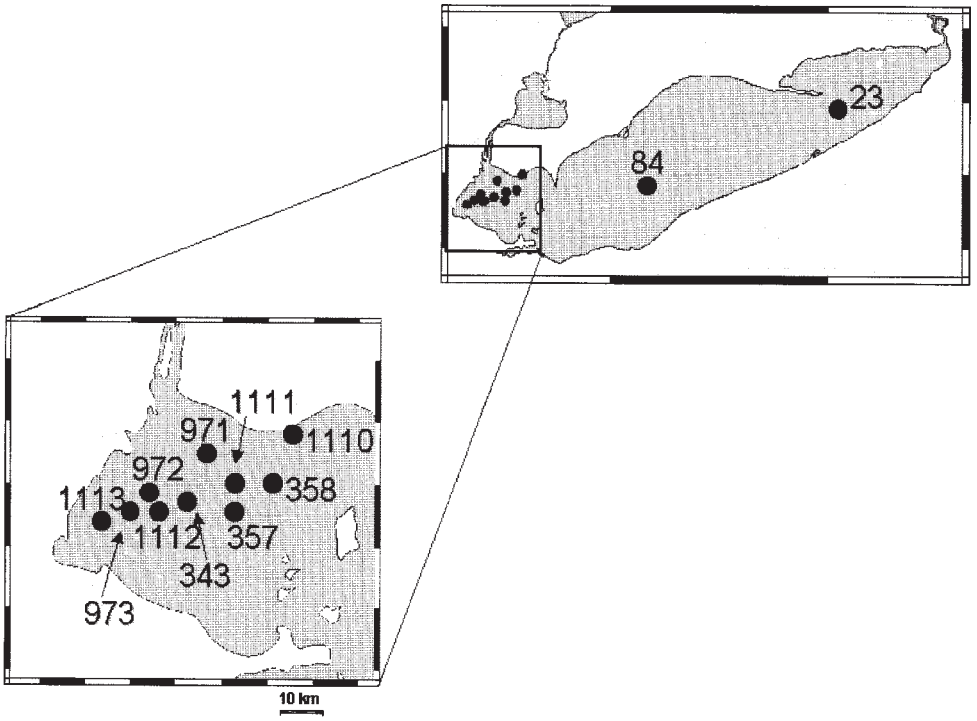

The impact of viruses on aquatic microorganisms should not be considered separately from the effects of solar radiation, since both viruses and bacteria are subject to damage by certain wavelengths and intensities of radiation (Wilhelm et al. 1998*a*, 1998*b*; Jeffrey et al. 1999). Moreover, both viruses and bacteria in aquatic environments are known to make use of some wavelengths of solar radiation for essential repair processes (Jeffery et al. 1999). Solar radiation effects are especially interesting in the Great Lakes due to recent increases in water clarity in many areas (e.g., Fahnenstiel et al. 1995) and simultaneous trends to higher surface incident fluxes of ultraviolet-B radiation (UVB) (280–320 nm) (Shindell et al. 1998). Solar radiation can also influence bacterial productivity through alterations in the bioavailability of organic substrates (e.g., Benner and Biddanda 1998; Tranvik and Kokalj 1998) and by altering the activity of potential bacterial consumers (Ochs 1997). The consequences of altered radiation exposure for microbial ecology are therefore complicated, but a logical starting point is to develop an understanding of the short-term inhibitory effects that are exerted directly on microorganisms. Although measurements in both marine and freshwater systems have documented significant impairment of bacterial productivity by UV and visible radiation exposure (e.g., Sommaruga et al. 1997; Jeffrey et al. 1999), estimates of photoinhibitory losses over meaningful depth and time scales are still impeded by lack of suitable models for describing the kinetics and spectral dependence of inhibition (cf. Neale et al. 1998*a*).

Our goals in this study were to test the hypothesis that viral-dependent mortality and photoinhibition are both important loss processes for bacterial production in Lake Erie and to estimate the relative magnitude of losses by each process. We present the first explicit models for estimating the impact of UV radiation on bacterial productivity in lakes and the first estimates for viral-dependent losses in this large lake. Our results are too few yet to fully characterize a system as large as Lake Erie, but they do provide important insight into the microbial ecology of the Great Lakes.

Materials and methods

Stations were occupied throughout the Lake Erie basin during research cruises in August 1997 and July 1998 (Fig. 1). Surface water samples were collected using 5-L Niskin bottles mounted on a rosette system. Temperature data were collected with the CTD equipment mounted on the rosette to model thermal stratification at each location. Additional casts were made with a SeaBird SBE-19 equipped with a SeaTech fluorometer to characterize the vertical distribution of chlorophyll *a* fluorescence. Total solar radiation was determined with an Eppley precision spectral pyranometer under Schott optical glass (WG295), which provides a linear spectral transparency to energy between 285 and 2800 nm. The device was linked to a Campbell recorder. Measurements, collected at 15-s increments, were integrated over 5-min periods for the duration of the cruise.

The abundance of virus-like particles was determined by Yo-Pro staining (Hennes and Suttle 1995) without prefiltration or DNase. Briefly, 50-μL water samples were collected throughout the solar day and diluted to 800 μL with virus-free (30 kDa filtered) water. Viruses were collected on 0.02-μm pore size ceramic filters (Anodisc 25, Whatman) and, after Yo-Pro staining, were enumerated with either an Olympus BX60 or an Olympus BH-2 epifluorescence microscope. Bacteria were enumerated in acridine orange treated water samples (2 mL) collected on 0.2-μm pore size black polycarbonate filters (Millipore GTBP) (Hobbie et al. 1977). The model of Murray and Jackson (1992) was used to calculate virus–host contact rates (per cell per day) as previously described (Wilhelm et al. 1998*a*).

The average number of viruses produced per bacterium lysed (burst size) was determined empirically by transmission electron

microscopy (Weinbauer and Peduzzi 1994). Bacteria from 10 mL of unfiltered, glutaraldehyde-preserved (2%, v/v) lake water were collected by centrifugation (3 h at 155 000 × *g*) on Formvar-coated, 400-mesh electron microscope grids and subsequently stained with 1% uranyl acetate. The frequency of visibly infected cells and burst sizes were estimated by counting the number of viral particles in visibly infected bacteria (as per Weinbauer and Peduzzi 1994) with a Philips EM 301 transmission electron microscope.

Bacterial carbon production and its response to solar radiation were measured in surface water samples, collected before 08:00, that had been placed in quartz tubes and exposed in deck boxes equipped with optical filters to create six different spectral treatments of natural solar radiation, ranging from full-spectrum to photosynthetically active radiation (PAR) (400–700 nm) only. UVB lamps (No. RPR-3000, Southern N.E. Ultraviolet Co., Brantford, Conn.) were used to increase incident UVB by about 50% in one additional treatment (160% when weighted for biological effectiveness by our July 8 weighting function), for a total of seven spectral treatments. Cellulose acetate was used on treatments receiving supplemental UVB to exclude any UV <280 nm. The other optical filter materials and their 50% transmission wavelengths were Mylar-D (320 nm), Hoya glass UV34 (340 nm), polystyrene (360 nm), and UF3 acrylic (400 nm, Cadillac Plastics, London, Ont.). Incident radiation spectra were recorded at approximately 30-min intervals throughout the photoperiod using an Oriel Instaspec radiometer as previously described (Smith et al. 1999). The spectral transmission characteristics in each treatment were also verified at the time of the experiments, using the same radiometer. Control samples were kept in darkness while the experimental exposures (1.5- to 5-h duration) were underway. Two experiments were performed at station 84 in July 1998.

Bacterial production was subsequently measured as the dark uptake of [^{3}H]thymidine (20 nM total added thymidine concentration) and [^{14}C]leucine (40 nM total concentration) in 1 h dual-label experiments (Chin-Leo and Kirchman 1988). Samples were collected via filtration through 0.22-μm nominal pore size mixed cellulose filters, extracted and rinsed with 5% TCA, and quantified by scintillation counting. Standard conversion factors were used to estimate bacterial carbon production from the substrate assimilation rates (Wetzel and Likens 1991). One substrate kinetics experiment at station 84 in July 1998 indicated that thymidine uptake was still unsaturated at 80 nM, and leucine at 160 nM, so the production estimates presented here are probably underestimates. A comparative experiment at station 84 did indicate, however, that uptake rates of each tracer were virtually identical whether measured in dual- or single-label experiments.

Two kinetic models were tested for their ability to describe the response of bacterial production rate to radiation exposure. Both are derived from recent work with phytoplankton. The first model (modified from Cullen et al. 1992; Neale et al. 1998*b*) postulates a rapid equilibrium between damage and repair:

$$(1) \qquad P(t)/P(\text{opt}) = 1/(1 + E^*)$$

where $P(t)$ is the instantaneous uptake rate after an exposure period t, $P(\text{opt})$ is the rate in the absence of photoinhibition, and E^* is the biologically weighted irradiance incident at time t (dimensionless). In application to bacteria assayed in the dark, the assumption would be that the degree of damage going into the period of tracer uptake would be proportional to the average irradiance prevailing during the experimental exposure and that repair in the dark would be negligible. There are grounds for the latter assumption, although it is not likely to be strictly true at the population level. The E^* is defined as

$$(2) \qquad E^* = \varepsilon_E(\text{PAR})E_{\text{PAR}} + \sum_{295}^{400} \varepsilon_E(\lambda)E(\lambda)\Delta\lambda$$

where $\varepsilon_E(\text{PAR})$ is the broad-band weighting (or effectiveness) coefficient for PAR irradiance and $\varepsilon_E(\lambda)$ is the spectral weighting coefficient for irradiance through the UV band from 295 nm (the shortest wavelength reaching the plankton in any significant amount) to 400 nm. Both coefficients are in the inverse of the irradiance units (joules per square metre per second).

The second model (modified from Neale et al. 1998*b*) postulates that repair is negligibly slow even in the light and takes the form

$$(3) \qquad P(t)/\text{P(opt)} = e^{-H^*}$$

where H^* is the cumulative biologically weighted radiation received up to time T:

$$(4) \qquad H^* = T\left[\varepsilon_H(\text{PAR})E_{\text{PAR}} + \sum_{295}^{400} \varepsilon_H(\lambda)E(\lambda)\Delta\lambda\right].$$

This assumes again that repair in the dark can be ignored but that the uptake rate will be proportional to the total number of damaging photons previously received and not the irradiance. The H^* is in the inverse of time-integrated irradiance units (joules per square metre). Both models were fit to the data by nonlinear, least squares regression using a derivative-free algorithm.

The values for $\varepsilon(\text{PAR})$ and $\varepsilon(\lambda)$ define the biological weighting function (BWF) and constitute the variable parameters that are estimated by fitting the kinetic models (eqs. 1 and 3). Following the procedure described in detail by Cullen and Neale (1997), we used principal components analysis to characterize the variation in spectral shape among our treatments, thus reducing the number of parameters to be estimated while avoiding a priori assumptions about the most appropriate functional form for the BWF. All statistical analyses were performed with Systat version 5 (Wilkinson 1992), and residuals analysis and plots were used to verify acceptable stability of variance and distribution of data.

Results and discussion

Viral distributions and inferred mortality

The western basin of Lake Erie was homogeneously mixed (z = 10 m) during sampling in August 1997. The abundance of free virus-like particles in the water column was high, ranging from 3.7×10^{10} to $37.9 \times 10^{10}\cdot L^{-1}$ (Table 1). In the central basin (station 84, July 1998), viral abundances were also homogeneously distributed through the water column in spite of a distinct thermocline at about 8 m (Table 2). The viral abundance in Lake Erie is similar to estimates from other freshwater systems, including Lake Constance (1.0×10^{10} to $4.0 \times 10^{10}\cdot L^{-1}$, Hennes and Simon 1995) and Lake Plußsee (1.0×10^{10} to $8.0 \times 10^{10}\cdot L^{-1}$, Weinbauer and Höfle 1998*a*), but higher than estimates for the more oligotrophic Lake Superior (1.5×10^9 to $9.2 \times 10^9\cdot L^{-1}$, Tapper and Hicks 1998). Viral abundance estimates in marine systems suggest that marine viral abundance is typically about one order of magnitude lower than those for Lake Erie (Maranger and Bird 1995; Wilhelm and Suttle 1999). Exceptions exist, however, and estimates of viral abundance in samples collected in the coastal waters of the western Gulf of Mexico (Wilhelm et al. 1998*a*) and from Long Island Sound (Proctor and Fuhrman 1990) are similar to our viral abundance estimates from Lake Erie.

Table 1. Distribution of bacteria and viruses across surface waters in the western basin of Lake Erie.

Station	Bacteria ($\times 10^9 \cdot L^{-1}$)		Viruses ($\times 10^{10} \cdot L^{-1}$)		VBR	Contacts ($cell^{-1} \cdot day^{-1}$)
	Mean	CV (%)	Mean	CV (%)		
23	3.1	28.0	6.1	9.2	19.5	7.2
343	2.6	9.6	7.5	4.7	29.2	5.9
357	3.2	8.8	3.7	42.2	11.5	7.4
358	3.2	21.1	15.2	47.3	47.4	7.4
971	4.6	8.9	5.4	4.7	11.8	10.5
972	2.2	22.8	5.2	34.6	23.8	5.0
973	2.5	12.7	9.0	7.2	35.4	5.9
1110	2.9	10.2	37.9	26.8	129.5	6.8
1111	3.8	25.9	11.1	42.3	29.0	8.8
1112	2.1	18.0	6.3	25.9	30.5	4.8
1113	2.1	1.7	9.0	9.0	42.7	4.9
1114	1.8	20.5	6.9	32.7	37.7	4.2

Note: Viruses and bacteria were enumerated (see text) and the VBR determined for each station. The frequency of virus–bacteria contacts (virus–bacterial collisions) per day was calculated using the equations of Murray and Jackson (1992) and subsequently corrected for total bacterial abundance to determine the frequency of contacts per cell (Wilhelm et al. 1998*a*).

Table 2. Distribution of virus-like particles through the water column at station 84.

Depth (m)	Viral abundance ($\times 10^{10} \cdot L^{-1}$)
1	6.5 (±0.4)
5	6.3 (±0.5)
10	7.3 (±0.7)
15	8.6 (±0.03)
20	7.0 (±1.4)

Note: Virus-like particles (±range, $n = 2$) were distributed ubiquitously through the water column in spite of a distinct thermocline at about 8 m.

Estimated bacterial abundance at various stations (Table 1) was similar to values determined for other freshwater environments (e.g., 1.2×10^9 to $18.3 \times 10^9 \cdot L^{-1}$ in Lake Superior, Tapper and Hicks 1998; 4.6×10^9 to $7.7 \times 10^9 \cdot L^{-1}$ in Lake Plußsee, Weinbauer and Höfle 1998*a*). The high viral abundance in Lake Erie provided for higher estimated virus to bacteria ratios (VBRs) and virus–bacteria contact rates (Table 1). In comparison, VBRs in Lake Superior ranged from only 0.03 to 0.53 across the water column. Microbial ecologists continue to debate the significance of calculating VBRs for aquatic systems; it has been suggested to loosely correlate with the trophic status of the system (Maranger and Bird 1995). High virus–host contact rates have been argued to suggest a high diversity of bacterial species and (or) resistant clones in the system (Wilhelm et al. 1998*a*).

Independent estimates of bacterial carbon production using [^{3}H]thymidine (1.74 ± 0.93 μg $C \cdot L^{-1} \cdot h^{-1}$) or [^{14}C]leucine ($1.26 \pm 0.05$ μg $C \cdot L^{-1} \cdot h^{-1}$) suggest that bacterial growth rate in the water column ranged from 0.6 to $0.8 \cdot day^{-1}$. It is difficult to determine why there is a discrepancy between these two independent estimates of bacterial production, but it may be related to the less-than-saturating substrate concentrations employed. Although these estimates can be viewed as underestimates of the bacterial carbon production rates, they imply that a virus-mediated turnover of carbon and nutrients was occurring in surface waters due to microbial activity. The bacterial growth rates estimated here would occupy the midrange of values reported for Lake Michigan during the stratified season (Scavia and Laird 1987).

As in other aquatic environments, bacterial carbon production in Lake Erie is sensitive to the activity of viruses. To estimate viral impacts on the bacterial community, samples were collected and subsequently examined by transmission electron microscopy. Samples from stations 343, 358, 973, and 1110 demonstrated a frequency of visible infected cells of 1.63% (SD = 0.59, $n = 12$). As cells are only visibly infected during the later stages of the lytic cycle, we employed the conversion factors of Proctor et al. (1993) to infer and model the proportion of bacterial mortality that was due to viral lysis. These conversion factors assume that infection and lysis occur at a constant rate, that infected cells are not grazed, and that viruses are visible within infected cells for about 14–27% of the lytic cycle. They also define mortality as twice the loss rate of bacterial destruction, based on the assumption that in a steady-state system, half of the daughter cells survive to divide. Using the conversion factors, our results suggest that 17.7% (12.1–23.4%) of the bacterial mortality in the western basin of Lake Erie was due to infection and subsequent lysis by phages. Under the assumption of an approximate steady state in bacterial biomass, the viral mortality therefore corresponds to approximately a 17.7% loss of productivity.

Burst sizes (determined by transmission electron microscopy) ranged from eight to 22 visible phages per infected cell (mean = 11.6). This is higher than those estimated for Lake Superior (about one) (Tapper and Hicks 1998) but significantly lower than burst sizes estimated in other freshwater systems (5–500, Weinbauer and Höfle 1998*b*). Combining the burst size estimates with bacterial turnover and viral abundance estimates, daily viral particle turnover in the western basin of Lake Erie was estimated at 5–13% (station 343), 3–8% (station 358), 4–11% (station 973), and 1–3% (station 1110). These viral turnover estimates are on the low end of estimates made in other systems (Kepner et al. 1998). Unlike the central basin of Lake Erie, however, the penetration of solar radiation into the western basin is rela-

Fig. 2. Leucine (open bars) and thymidine (solid bars) assimilation rates in station 84 water preexposed to full-spectrum solar radiation (>290), PAR + UVA only (>320), PAR + long UVA only (>340), or full-spectrum plus supplementary UVB (+UVB) for 3.5 h at 50% of incident as percentages of rates in water preexposed to PAR only. DARK denotes water kept in darkness. Bars are standard deviations for triplicates.

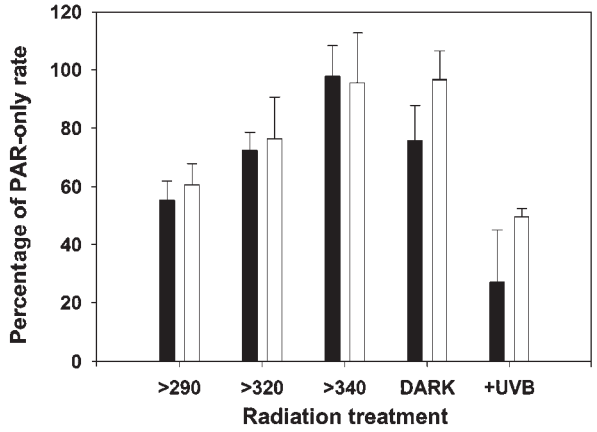

tively low, in part due to a high load of suspended particulate material (Smith et al. 1999). As sunlight appears to be the major mechanism of viral destruction in aquatic systems (see Wilhelm et al. 1998*a*, 1998*b*; Jeffrey et al. 1999), this implies that a limited decay of viruses in this system would occur. Thus, in combination with the high concentration of viral particles in the basin, our results suggest that only a minimal turnover of the total viral population is required to maintain a significant mortality (17.7% as per above) of the bacterial community.

UV radiation effects on bacterial activity

In the radiation exposure experiments at station 84 in July 1998, water preexposed to PAR only consistently supported equivalent or higher bacterial productivity compared with control water kept in the dark (e.g., Fig. 2). PAR has previously been reported in other lakes to inhibit bacterial production at some sites and depths but not at others (Sommaruga et al. 1997), and its role will probably depend on the severity of the exposure and properties of the plankton assemblage. Under our experimental conditions, we observed no PAR-dependent inhibition, so the PAR-only treatments were used to define $P(\text{opt})$.

Full-spectrum exposures at 50% of incident radiation for 1.5–5 h caused $P(t)/P(\text{opt})$, the ratio of inhibited to optimal production rate, to decrease by 40–60% whether assessed by thymidine or leucine assimilation (e.g., Fig. 2). The degree of inhibition prevalent in the irradiated sample may have been even larger insofar as some recovery may have occurred during the uptake experiments, but in darkness the degree of recovery would probably not be very great within the 1-h time period concerned (Kaiser and Herndl 1997). A significant portion of the apparent inhibition was due to UVB (280–320 nm), but UVA (320–400 nm) also appeared to be inhibitory.

Both of the kinetic models (eqs. 1 and 3) that we investigated explained a significant amount of variation in $P(t)/P(\text{opt})$. However, the irradiance-dependent model (eq. 1)

Fig. 3. Bacterial productivity in radiation-exposed treatments relative to optimal, noninhibited productivity for the experiment of July 9 at station 84 and exposures of 1.5 h (circles) or 4 h (triangles). Solid lines show prediction of the (A) irradiance-dependent model (eq. 1) and the (B) exposure-dependent model (eq. 3). The percent explained variation was 48% for the irradiance-dependent model and 80% for the exposure-dependent model.

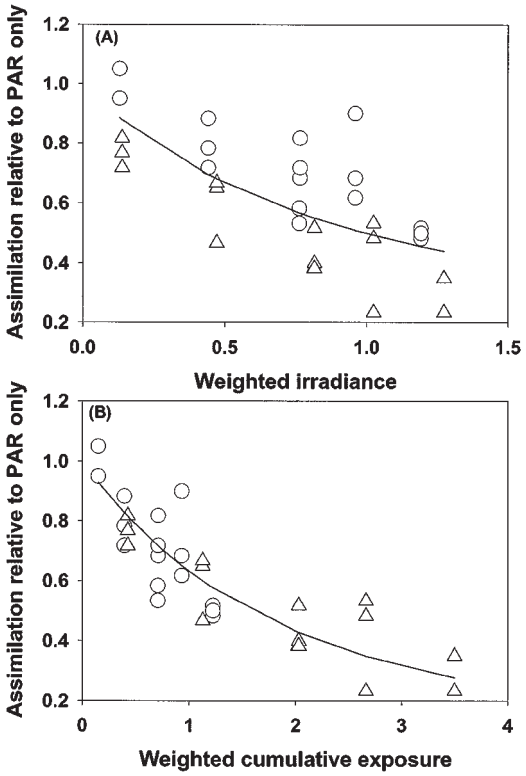

displayed systematic error in its predictions, underestimating the degree of photoinhibition in shorter exposures and overestimating it in longer exposures (Fig. 3). A *t* test of the residuals for short versus longer exposures confirmed a significant ($p < 0.01$) difference and thus a systematic lack of fit. This differs from experience with laboratory cultures of diatoms (Cullen et al. 1992), which conform well to the model, but is similar to problems others have had in using the model to describe the kinetics of phytoplankton photoinhibition in the Antarctic (Neale et al. 1998*b*) and in Lakes Erie and Ontario (Smith et al. 1998; V. Hiriart and R. Smith, unpublished data).

In most of those cases in which the irradiance-dependent model has failed to account for phytoplankton responses, the cumulative exposure model provided much better fit to the data (Neale et al. 1998*b*; Smith et al. 1998). The implication would appear to be that the rate of DNA repair is slow compared with the rate of DNA damage in natural phytoplankton communities. In the present case, the cumulative exposure model (eq. 3) provided good fit to the data, particularly in the sense that systematic lack of fit among treatments was very slight (Fig. 3). The residuals for short versus longer incubations were not significantly different ($p > 0.1$), confirming the apparent systematic lack of fit as a function of exposure period. We therefore suggest that repair was slow compared with damage during the experimental exposures of

Table 3. Values of the biological weighting coefficients $\varepsilon_H(\lambda)$ and $\varepsilon_H(\mathrm{PAR})$ ($m^2 \cdot J^{-1}$) for both thymidine and leucine assimilation by Lake Erie bacterioplankton on two dates in 1998 at station 84.

Wavelength (nm)	Biological weighting coefficients			
	July 8		July 9	
	Thymidine	Leucine	Thymidine	Leucine
295.484	3.14×10^{-4}	1.67×10^{-4}	2.31×10^{-3}	2.54×10^{-3}
297.518	2.88×10^{-4}	1.59×10^{-4}	2.01×10^{-3}	2.22×10^{-3}
299.552	2.56×10^{-4}	1.52×10^{-4}	1.34×10^{-3}	1.48×10^{-3}
301.585	2.59×10^{-4}	1.57×10^{-4}	9.24×10^{-4}	1.02×10^{-3}
303.617	2.20×10^{-4}	1.40×10^{-4}	4.24×10^{-4}	4.68×10^{-4}
305.649	2.14×10^{-4}	1.42×10^{-4}	2.55×10^{-4}	2.84×10^{-4}
307.681	1.86×10^{-4}	1.28×10^{-4}	1.61×10^{-4}	1.79×10^{-4}
309.712	1.68×10^{-4}	1.19×10^{-4}	1.20×10^{-4}	1.33×10^{-4}
311.742	1.25×10^{-4}	9.05×10^{-5}	7.55×10^{-5}	8.41×10^{-5}
313.772	1.13×10^{-4}	8.21×10^{-5}	6.76×10^{-5}	7.52×10^{-5}
315.801	1.07×10^{-4}	8.04×10^{-5}	5.94×10^{-5}	6.73×10^{-5}
317.829	9.25×10^{-5}	7.11×10^{-5}	5.21×10^{-5}	6.05×10^{-5}
319.857	8.59×10^{-5}	6.73×10^{-5}	4.47×10^{-5}	5.31×10^{-5}
321.885	7.90×10^{-5}	6.28×10^{-5}	3.90×10^{-5}	4.71×10^{-5}
323.912	7.17×10^{-5}	5.77×10^{-5}	3.41×10^{-5}	4.17×10^{-5}
325.938	5.71×10^{-5}	4.61×10^{-5}	2.62×10^{-5}	3.23×10^{-5}
327.964	4.66×10^{-5}	3.78×10^{-5}	2.07×10^{-5}	2.57×10^{-5}
329.990	4.13×10^{-5}	3.35×10^{-5}	1.83×10^{-5}	2.27×10^{-5}
332.015	4.05×10^{-5}	3.29×10^{-5}	1.88×10^{-5}	2.35×10^{-5}
334.039	4.00×10^{-5}	3.25×10^{-5}	2.04×10^{-5}	2.58×10^{-5}
336.063	3.86×10^{-5}	3.12×10^{-5}	2.14×10^{-5}	2.73×10^{-5}
338.086	3.50×10^{-5}	2.84×10^{-5}	2.29×10^{-5}	2.96×10^{-5}
340.108	2.69×10^{-5}	2.17×10^{-5}	2.00×10^{-5}	2.60×10^{-5}
342.130	2.20×10^{-5}	1.77×10^{-5}	1.96×10^{-5}	2.58×10^{-5}
344.152	1.95×10^{-5}	1.56×10^{-5}	1.99×10^{-5}	2.64×10^{-5}
346.173	1.48×10^{-5}	1.18×10^{-5}	1.91×10^{-5}	2.56×10^{-5}
348.193	1.14×10^{-5}	8.90×10^{-6}	1.84×10^{-5}	2.48×10^{-5}
350.213	8.60×10^{-6}	6.60×10^{-6}	1.69×10^{-5}	2.29×10^{-5}
352.233	5.90×10^{-6}	4.50×10^{-6}	1.60×10^{-5}	2.18×10^{-5}
354.251	4.10×10^{-6}	3.00×10^{-6}	1.47×10^{-5}	2.01×10^{-5}
356.270	3.20×10^{-6}	2.30×10^{-6}	1.47×10^{-5}	2.01×10^{-5}
358.287	3.40×10^{-6}	2.40×10^{-6}	1.76×10^{-5}	2.42×10^{-5}
360.305	2.00×10^{-7}	1.16×10^{-8}	1.45×10^{-5}	2.00×10^{-5}
362.321	2.00×10^{-7}	1.13×10^{-8}	1.43×10^{-5}	1.97×10^{-5}
364.337	-2.00×10^{-6}	-2.00×10^{-6}	1.25×10^{-5}	1.74×10^{-5}
366.353	-3.00×10^{-6}	-2.00×10^{-6}	1.09×10^{-5}	1.52×10^{-5}
368.368	-2.00×10^{-6}	-2.00×10^{-6}	1.08×10^{-5}	1.51×10^{-5}
370.382	-2.00×10^{-6}	-2.00×10^{-6}	1.03×10^{-5}	1.43×10^{-5}
372.396	-3.00×10^{-6}	-2.00×10^{-6}	1.11×10^{-5}	1.55×10^{-5}
374.410	-3.00×10^{-6}	-2.00×10^{-6}	1.27×10^{-5}	1.78×10^{-5}
376.422	-3.00×10^{-6}	-3.00×10^{-6}	1.11×10^{-5}	1.55×10^{-5}
378.435	-3.00×10^{-6}	-2.00×10^{-6}	9.30×10^{-6}	1.30×10^{-5}
380.446	-4.00×10^{-6}	-3.00×10^{-6}	1.03×10^{-5}	1.45×10^{-5}
382.457	-4.00×10^{-6}	-3.00×10^{-6}	1.28×10^{-5}	1.80×10^{-5}
384.468	-7.00×10^{-6}	-5.00×10^{-6}	1.37×10^{-5}	1.92×10^{-5}
386.478	-6.00×10^{-6}	-4.00×10^{-6}	1.17×10^{-5}	1.64×10^{-5}
388.488	-6.00×10^{-6}	-5.00×10^{-6}	1.13×10^{-5}	1.59×10^{-5}
390.497	-6.00×10^{-6}	-4.00×10^{-6}	9.40×10^{-6}	1.33×10^{-5}
392.505	-6.00×10^{-6}	-4.00×10^{-6}	1.09×10^{-5}	1.53×10^{-5}
394.513	-6.00×10^{-6}	-4.00×10^{-6}	1.18×10^{-5}	1.66×10^{-5}
396.520	-6.00×10^{-6}	-5.00×10^{-6}	1.07×10^{-5}	1.50×10^{-5}
398.527	-5.00×10^{-6}	-4.00×10^{-6}	8.60×10^{-6}	1.21×10^{-5}
PAR (400–700)	-4.70×10^{-8}	-3.40×10^{-8}	2.00×10^{-7}	1.80×10^{-7}

Fig. 4. Weighting coefficient spectra (BWFs) normalized to unity at 300. Spectra for thymidine assimilation on July 8 and July 9 from the present study (spectra for leucine were nearly identical) and spectra from the literature for chloroplast inhibition (Jones and Kok 1966) and photoinhibition of a marine diatom (Cullen et al. 1992) and the DNA action spectrum of Setlow (1974). (A) Entire range defined in the present study; (B) enlargement of the UVA portion of the spectrum.

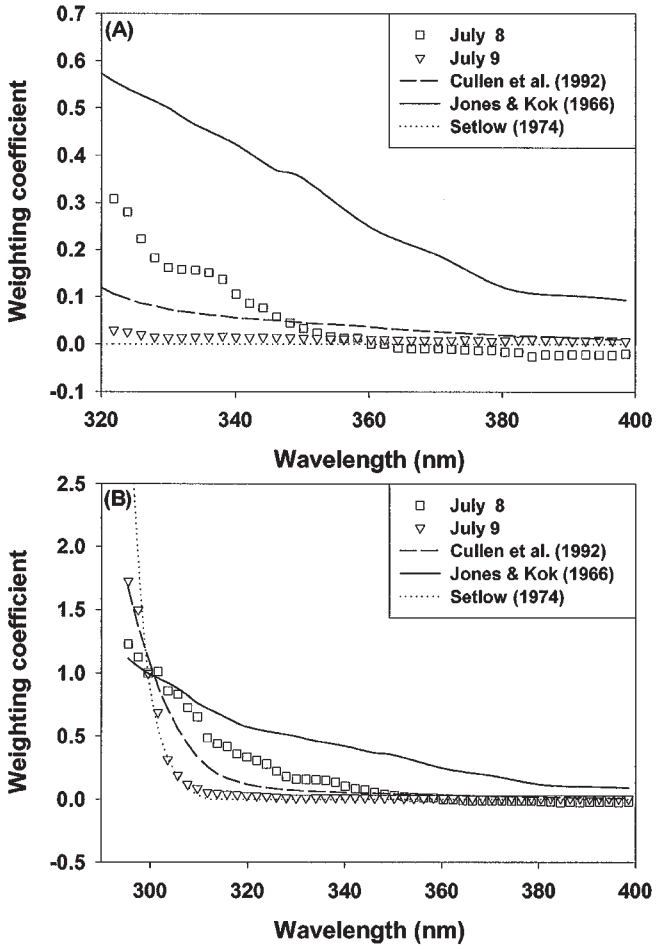

the bacterial assemblages at station 84. This seems reasonable, as DNA damage has been shown to accumulate in various size-classes of marine organisms (viruses and bacteria) through the solar day in spite of DNA repair systems (see Jeffrey et al. 1999).

BWFs were derived for two experiments performed on successive days at station 84. The weighting functions do not have a convenient analytical form, so we list the values for each day and substrate to facilitate their application by other investigators (Table 3). Insofar as thymidine assimilation is primarily a measure of nucleic acid synthesis, while leucine assimilation is primarily a measure of protein synthesis, we had entertained the hypothesis that the two processes might have rather different spectral responses to UV radiation. In fact, the BWFs for assimilation of the two substrates were nearly identical (Table 3), and we plot here only those for thymidine assimilation (Fig. 4). By comparison, BWFs for processes known to be mediated by different primary damage sites, such as DNA lesion induction (Setlow 1974) versus chloroplast inhibition (Jones and Kok 1966), are distinctly different from each other in shape (Fig. 4). It would appear that nucleic acid and protein synthesis in the

Fig. 5. Whole solar spectral energy for July 7–9 at station 84 (courtesy of R. Bourbonniere, unpublished data). Total solar spectral energy was collected as described in the Materials and methods. Results demonstrate increasing levels of solar radiation at station 84 over the period of the experiment as well as for the prior 24 h.

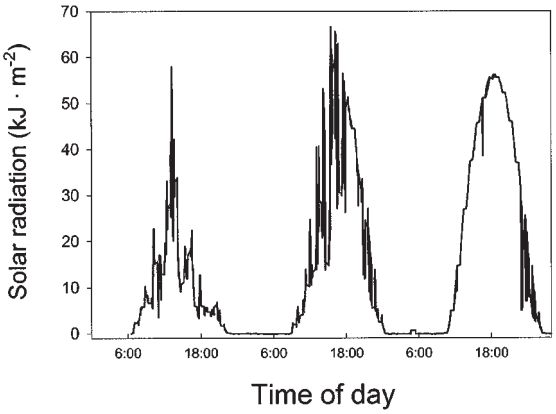

Fig. 6. Temperature (thick line, circles) and in situ fluorescence (thin line) profiles for (A) 06:30 and (B) 18:30 on July 8, 1998, at station 84.

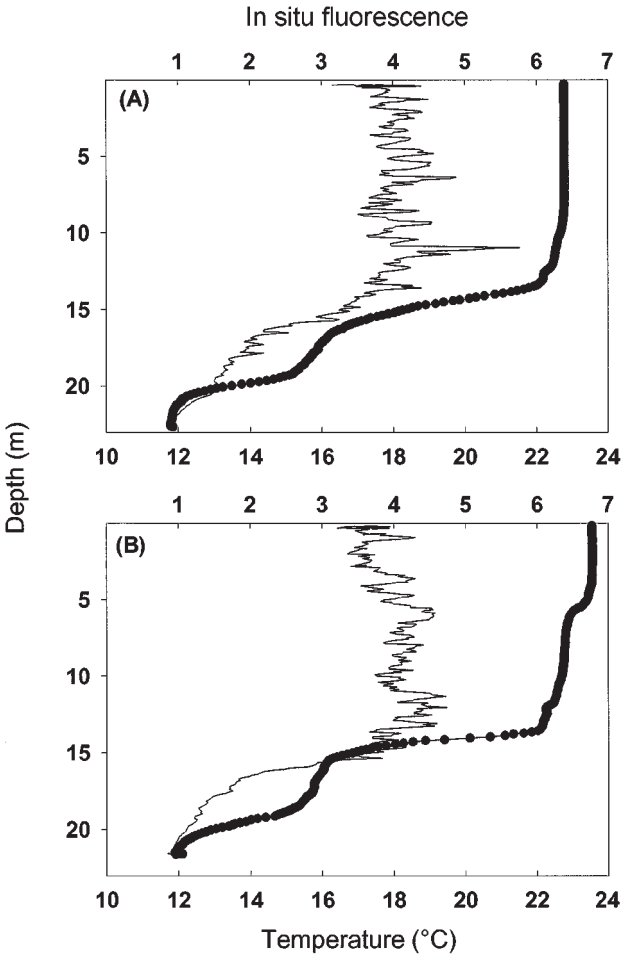

Fig. 7. Biologically weighted radiation spectra for (A) July 8 and (B) July 9, 1999. Biologically effective radiation spectra (i.e., the dimensionless cross-product of biological weighting coefficients, ε_H, for thymidine assimilation (Table 3) and spectral radiation) just under the surface (0 m) and at 0.5 and 1.0 m depths for median conditions of water clarity and clear skies in Lake Erie.

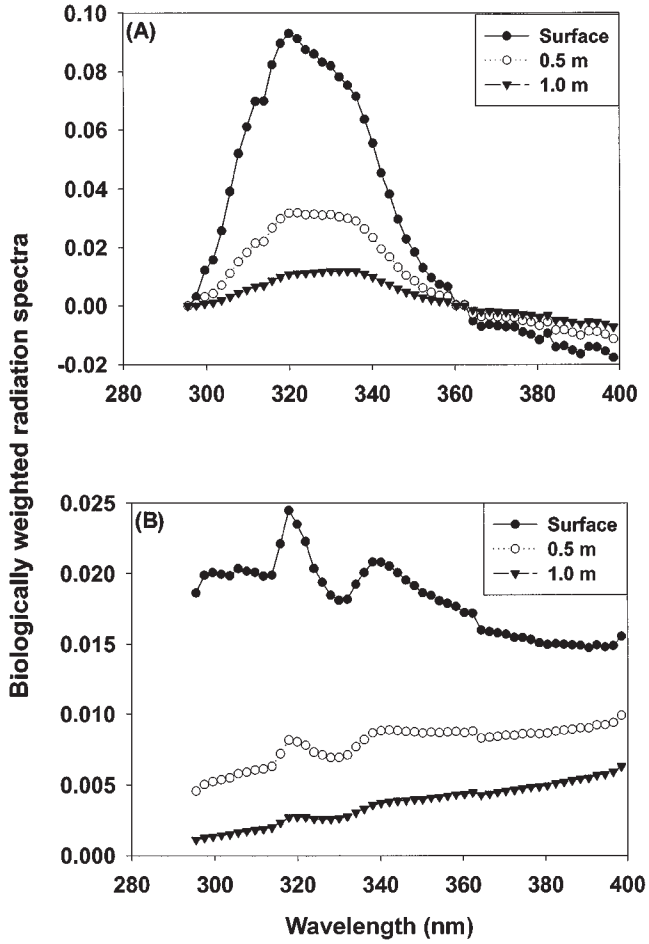

Lake Erie bacterial assemblages that we encountered were responding to some common site, or sites, of proximate damage.

The BWFs, although similar for the two substrates, differed considerably between the two days of experimentation (Table 3; Fig. 4). BWFs measured by the same method used here, but for phytoplankton, also vary among phytoplankton communities sampled on different days and at different sites in the Weddell–Scotia Sea near Antarctica (Neale et al. 1998*b*). The variation of the phytoplankton BWFs could be explained in terms of varying physiological condition related to differing water column stability and light climate, among other environmental factors (Neale et al. 1998*b*). Variations in BWF shape even greater than those reported from Antarctica have been observed for phytoplankton at different sites and months in Lake Erie (V. Hiriart, unpublished data).

In the present case, the first BWF (July 8) was measured on the first clear day consequent to several days of overcast weather, while the second (July 9) was measured on plankton that had presumably received considerable radiation exposure over the previous photoperiod (Fig. 5). Profiles of temperature and in vivo chlorophyll *a* fluorescence (e.g., Fig. 6) showed a distinct loss of fluorescence from beginning to end of the photoperiod on both days in the upper 5 m and the formation of a diurnal thermocline at approximately 5 m depth. Winds were light over the 48-h study period, allowing such temporary stratification to develop each day. Thus, the plankton sampled on July 9 may well have been altered by the previous day's exposure. There was no evidence for advection of a different water mass into the study area between the two days, insofar as gross water column properties (temperature, chlorophyll *a* concentration, PAR attenuation, and major nutrient concentrations) were unchanged. Without further measurements, we would not conclude that such large variations in BWFs on such short time scales are typical, but we do suggest that UV radiation impact on bacterial communities will not be accurately modeled with a constant, universal BWF.

The cumulative exposure model (eq. 3) and its weighting functions (Table 3) were combined with the measured incident radiation spectra and information about spectral transmissivity of the water column to illustrate the changing spectral contributions to photoinhibition with depth and to generate estimates of depth- and time-integrated photoinhibition. Spectral transmission was unfortunately not measured at the time of the experiments, but systematic surveys in 1997 showed that spectral transmission through the UV waveband was usefully predictable from knowledge of the attenuation coefficient (k) at 320 nm (Smith et al. 1999). For illustrative purposes, we adopted the 1997 median Lake Erie value of $k_{320} = 2.1 \cdot m^{-1}$ and a corresponding value of $k_{PAR} = 0.9 \cdot m^{-1}$; actual values for the central basin in summer are usually lower, so the inhibition estimates given here are correspondingly conservative for station 84.

The cross-product of the weighting coefficients (Table 3) and the ambient spectral radiation defines the biologically effective radiation spectrum (dimensionless) and illustrates the spectral contributions to photoinhibition and their variation with depth (Fig. 7). Although the weighted radiation spectra varied strongly between days, they showed a common trend to increased relative importance of UVA with increasing depth, a consequence of the more rapid attenuation of UVB than UVA with depth. The contrast between days is even more apparent in Fig. 7 than in Fig. 4. On July 8, short UVA was inhibitory but long UVA was benign or even beneficial. On July 9, both short and long UVA were apparently inhibitory. Although it is tempting to assume that effects on protein synthesis must follow from primary effects on nucleic acids, the substantial inhibitory weighting given to the UVA band in both experiments was not consistent with the idea that nucleic acids were the only primary site of effect. Our results thus confirm and quantify previous observations that UVA is the major (or even dominant) agent of bacterial photoinhibition and point to the importance of damage sites other than nucleic acids in natural bacterial assemblages. Those "sites" could conceivably include other organisms such as phytoplankton, which are important to the nutrition of bacterioplankton and which modify bacterial response to UV radiation (e.g., Sommaruga et al. 1997). Observations such as ours on entire communities of organisms cannot always be interpreted in purely physiological terms.

Given the evidence (Fig. 6) for limited mixing in the

Table 4. Loss of bacterial productivity (as a percentage of the nonphotoinhibited value) over one photoperiod and two different integration depths at station 84 as predicted by the fitted BWFs and exposure-dependent model for median conditions of water clarity and a static water column.

Integration depth (m)	Wavebands contributing (nm)	Thymidine	Leucine
5	295–400 (UVB + UVA)	16–25	14–30
5	295–320 (UVB only)	1.5–3.5	1.2–3.0
10	295–400 (UVB + UVA)	8–13	7–15
10	295–320 (UVB only)	0.8–1.7	0.6–1.5

Note: For each substrate (thymidine and leucine), the lower end of the inhibition range is the prediction from the July 8 BWF and the higher is from the July 9 BWF.

epilimnion during the photoperiod, we adopted a static water column model (Neale et al. 1998*a*) to calculate time- and depth-integrated photoinhibition. Photoinhibition in each depth stratum over the photoperiod was accordingly proportional to the time-integrated weighted radiation received at that depth. It was then necessary only to integrate over the appropriate depth range to calculate the column-integrated photoinhibition. Based on the observed thermal and fluorescence structure, there appeared to be two logical integration depths of interest, the first being the diurnal mixed layer depth of about 5 m and the second being the seasonal mixed layer depth of about 10 m.

The predicted photoinhibition was very similar whether production was estimated by thymidine or leucine assimilation (Table 4). The July 8 BWF predicted less inhibition than did the July 9 BWF. The inhibition was due entirely to UV, not PAR. UVA (320–400 nm) was the dominant inhibitory waveband, with UVB causing only a few percent loss at most. Predicted inhibition was greater over the 5- than the 10-m integration depth because there was almost no UV effect below 5 m. Like some earlier estimates (Sommaruga 1997), our model calculations show that UV-dependent photoinhibition in the epilimnion is likely to be appreciable. Unlike earlier estimates for bacteria, ours use models that provide an explicit basis for interpreting the implications of altered water clarity and (or) incident radiation. For example, we can point out that with more typical summer values for spectral transmission in the offshore central basin (k_{320} = $1.8 \cdot m^{-1}$ and k_{PAR} = $0.3 \cdot m^{-1}$), station 84 would be subject over the course of one photoperiod to about 50% photoinhibitory loss of bacterial production over 5 m and 25% over 10 m if the BWFs derived here were applicable. If, as many think, Lake Erie is continuing on a trend to greater water clarity because of *Dreissena* activity and continued nutrient loading controls, then increased photoinhibitory losses may indeed be appreciable.

A great deal more work is needed before we can realistically evaluate the full role of UV radiation in the microbial ecology of Lake Erie and other aquatic systems. Not only do we need additional measurements to characterize and predict the variability of bacterial BWFs and kinetic responses, we also need to account for events outside the photoperiod and below the photic zone (e.g., cell repair and photochemical substrate generation) that can influence bacterial production (e.g., Kaiser and Herndl 1997). UV radiation could potentially stimulate additional bacterial productivity if appropriate depth and time scales are chosen, through such mechanisms as liberation of labile substrates (e.g., Lindell et al. 1995) and inhibition of viruses (Wilhelm et al. 1998*a*) or bacterivores (Ochs 1997). What we have presented here is the means to assess the relatively direct and short-term effects of UV radiation on the bacterial community. While we, and others (e.g., Neale et al. 1998*a*), would argue that such means are a necessary prerequisite, they are certainly not the full solution to the problem of predicting the impact of a changing UV environment on aquatic ecosystems.

Conclusions

In this study, we have examined two independent mechanisms that directly influence bacterial productivity. Viruses and UV caused decreases of comparable magnitude in bacterial productivity over one photoperiod in the surface mixed layer in the present case. The effects are, however, mediated by different mechanisms. Lytic viruses remove bacteria from the system by destroying the bacterium during lysis, leading to direct increases in bacterial mortality and thus loss of potential production. Although UV radiation can also physically disrupt bacteria, it functions to inactivate bacteria by causing damage to cellular machinery, leading to losses in productivity. UV-mediated productivity loses are, however, reversible (at some level) by light-dependent and -independent DNA repair mechanisms (Sancar 1994; Jeffrey et al. 1999). The results of this study demonstrate the underlying complexity of the microbial ecology of aquatic systems. They also demonstrate the need for future work on aquatic systems with an integrated approach to the multiple interactions that exist.

Acknowledgments

We thank Robert Hecky for providing space on his cruise in August of 1997 and Chris Allen, Rick Bourbonniere, Scott Kirby, Nancy Lane, and the captain, crew, and technical operations staff of the CCGS *Limnos* for assistance in the collection and processing of samples. We are also indebted to Curtis Suttle for providing access to electron microscopic facilities. The suggestions of John Cullen, Markus Weinbauer, and an anonymous reviewer improved the manuscript. This work was supported by grants from Environment Canada (S.W.W. and R.E.H.S.), the Great Lakes 2000 fund (S.W.W. through Environment Canada), the National Science Foundation (S.W.W.), and the Natural Sciences and Engineering Research Council of Canada (R.E.H.S.).

References

Benner, R., and Biddanda, B. 1998. Photochemical transformations of surface and deep marine dissolved organic matter: effects on bacterial growth. Limnol. Oceanogr. **43**: 1373–1378.

Chin-Leo, G., and Kirchman, D.L. 1988. Estimating bacterial production in marine waters from the simultaneous incorporation of thymidine and leucine. Appl. Environ. Microbiol. **54**: 1934–1939.

Cullen, J.J., and Neale, P.J. 1997. Biological weighting functions for describing the effects of ultraviolet radiation on aquatic systems. *In* The effects of ozone depletion on aquatic ecosystems. *Edited by* D.P. Hader. R.G. Landes Co., New York. pp. 97–118.

Cullen, J.J., Neale, P.J., and Lesser, M.P. 1992. Biological weighting function for the inhibition of phytoplankton photosynthesis by ultraviolet radiation. Science (Washington, D.C.), **258**: 646–650.

Fahnenstiel, G.L., Land, G.A., Nalepa, T.F., and Johengen, T.H. 1995. Effects of zebra mussel (*Dreissena polymorpha*) colonization on water quality parameters in Saginaw Bay, Lake Huron. J. Gt. Lake Res. **21**: 435–448.

Hennes, K.P., and Simon, M. 1995. Significance of bacteriophage for controlling bacterioplankton growth in a mesotrophic lake. Appl. Environ. Microbiol. **61**: 333–340.

Hennes, K.P., and Suttle, C.A. 1995. Direct counts of viruses in natural waters and laboratory cultures by epifluorescence microscopy. Limnol. Oceanogr. **40**: 1050–1055.

Hobbie, J.E., Daley, R.J., and Jasper, S. 1977. Use of nucleopore filters for counting bacteria by fluorescence microscopy. Appl. Environ. Microbiol. **33**: 1225–1228.

Jeffrey, W.H., Kase, J.P., and Wilhelm, S.W. 1999. Ultraviolet radiation effects on bacterioplankton and viruses in marine ecosystems. *In* Effects of UV radiation on marine ecosystems. *Edited by* S.E. De Mora. Cambridge University Press, Cambridge, U.K. In press.

Jones, L.W., and Kok, B. 1966. Photoinhibition of chloroplast reactions. Kinetics and action spectra. Plant Physiol. **41**: 1037–1043.

Kaiser, E., and Herndl, G.J. 1997. Rapid recovery of marine bacterioplankton activity after inhibition by UV radiation in coastal waters. Appl. Environ. Microbiol. **63**: 4026–4031.

Kepner, R.L., Wharton, R.A., and Suttle, C.A. 1998. Viruses in Antarctic lakes. Limnol. Oceanogr. **43**: 1754–1761.

Lindell, M.J., Graneli, W., and Tranvik, L.J. 1995. Enhanced bacterial growth in response to photochemical transformation of dissolved organic matter. Limnol. Oceanogr. **40**: 195–199.

Maranger, R., and Bird, D.F. 1995. Viral abundance in aquatic systems: a comparison between marine and fresh waters. Mar. Ecol. Prog. Ser. **121**: 217–226.

Mortimer, C.H. 1987. Fifty years of physical investigations and related limnological studies on Lake Erie, 1928–1977. J. Gt. Lake Res. **13**: 407–435.

Murray, A.G., and Jackson, G.A. 1992. Viral dynamics: a model of the effects of size, shape, motion and abundance of single-celled planktonic organisms and other particles. Mar. Ecol. Prog. Ser. **89**: 103–116.

Neale, P.J., Davis, R.F., and Cullen, J.J. 1998*a*. Interactive effects of ozone depletion and vertical mixing on photosynthesis of Antarctic phytoplankton. Nature (Lond.), **392**: 585–589.

Neale, P.J., Cullen, J.J., and Davis, R.F. 1998*b*. Inhibition of marine photosynthesis by ultraviolet radiation: variable sensitivity of phytoplankton in the Weddell–Scotia Confluence during the austral spring. Limnol. Oceanogr. **43**: 433–448.

Nicholls, K.H., and Hopkins, G.J. 1993. Recent changes in Lake Erie (north shore) phytoplankton: cumulative impacts of phosphorus loading reductions and the zebra mussel introduction. J. Gt. Lakes Res. **19**: 637–647.

Ochs, C.A. 1997. Effects of UV radiation on grazing by two marine heterotrophic nanoflagellates on autotrophic picoplankton. J. Plankton Res. **19**: 1517–1536.

Proctor, L.M., and Fuhrman, J.A. 1990. Viral mortality of marine bacteria and cyanobacteria. Nature (Lond.), **343**: 60–62.

Proctor, L.M., Okubo, A., and Fuhrman, J.A. 1993. Calibrating estimates of phage-induced mortality in marine bacteria: ultrastructural studies of marine bacteriophage development from one-step growth experiment. Microb. Ecol. **25**: 161–182.

Sancar, A. 1994. Mechanisms of DNA excision repair. Science (Washington, D.C.), **266**: 1954–1956.

Scavia, D.L., and Laird, G.A. 1987. Bacterioplankton in Lake Michigan: dynamics, controls and significance to carbon flux. Limnol. Oceanogr. **32**: 1017–1033.

Setlow, R.B. 1974, The wavelengths in sunlight effective in producing skin cancer: a theoretical analysis. Proc. Natl. Acad. Sci. U.S.A. **71**: 3363–3366.

Shindell, D., Rind, D., and Lonergan, P. 1998. Increased polar stratospheric ozone losses and delayed eventual recovery owing to increasing greenhouse-gas concentrations: Nature (Lond.), **392**: 589–592.

Smith, R.E.H., Furgal, J.A., and Lean, D.R.S. 1998. The short-term effects of solar ultraviolet radiation on phytoplankton photosynthesis and photosynthate allocation under contrasting mixing regimes in Lake Ontario. J. Gt. Lake Res. **24**: 427–441.

Smith, R.E.H., Furgal, J.A., Charlton, M.N., Greenberg, B.M., Hiriart, V., and Marwood, C. 1999. Attenuation of ultraviolet radiation in a large lake with low dissolved organic matter concentrations. Can. J. Fish. Aquat. Sci. **56**: 1351–1361.

Sommaruga, R., Obernosterer, I., Herndl, G.J., and Psenner, R. 1997. Inhibitory effect of solar radiation on thymidine and leucine incorporation by freshwater and marine bacterioplankton. Appl. Environ. Microbiol. **63**: 4178–4184.

Tapper, M.A., and Hicks, R.E. 1998. Temperate viruses and lysogeny in Lake Superior bacterioplankton. Limnol. Oceanogr. **43**: 95–103.

Tranvik, L., and Kokalj, S. 1998. Decreased biodegradability of algal DOC due to interactive effects of UV radiation and humic matter. Aquat. Microb. Ecol. **14**: 301–307.

Weinbauer, M.G., and Höfle, M.G. 1998*a*. Size-specific mortality of lake bacterioplankton by natural virus communities. Aquat. Microb. Ecol. **15**: 103–113.

Weinbauer, M.G., and Höfle, M.G. 1998*b*. Significance of viral lysis and flagellate grazing as controlling factors of bacterioplankton production in an eutrophic lake. Appl. Environ. Microbiol. **64**: 431–438.

Weinbauer, M.G., and Peduzzi, P. 1994. Frequency, size and distribution of bacteriophages in different marine morphotypes. Mar. Ecol. Prog. Ser. **108**: 11–20.

Wetzel, R.G., and Likens, G.E. 1991. Limnological methods. Springer-Verlag, New York.

Wilhelm, S.W., and Suttle, C.A. 1999. Viruses and nutrient cycles in the sea. BioScience, **49**: 781–788.

Wilhelm, S.W., Weinbauer, M.G., Suttle, C.A., and Jeffrey, W.H. 1998*a*. The role of sunlight in the removal and repair of viruses in the sea. Limnol. Oceanogr. **43**: 586–592.

Wilhelm, S.W., Weinbauer, M.G., Suttle, C.A., Pledger, R.J., and Mitchell, D.L. 1998*b*. Measurements of DNA damage and photoreactivation imply that most viruses in marine surface waters are infective. Aquat. Microb. Ecol. **14**: 215–222.

Wilkinson, L. 1992. Systat for Windows, version 5. Systat, Inc., Evanston, Ill.